

Supplementary Materials for

Retinol binding protein 3 is increased in the retina of patients with diabetes resistant to diabetic retinopathy

Hisashi Yokomizo, Yasutaka Maeda, Kyoungmin Park, Allen C. Clermont, Sonia L. Hernandez, Ward Fickweiler, Qian Li, Chih-Hao Wang, Samantha M. Paniagua, Fabricio Simao, Atsushi Ishikado, Bei Sun, I-Hsien Wu, Sayaka Katagiri, David M. Pober, Liane J. Tinsley, Robert L. Avery, Edward P. Feener, Timothy S. Kern, Hillary A. Keenan, Lloyd Paul Aiello, Jennifer K. Sun, George L. King*

*Corresponding author. Email: george.king@joslin.harvard.edu

Published 3 July 2019, *Sci. Transl. Med.* **11**, eaau6627 (2019)
DOI: 10.1126/scitranslmed.aau6627

The PDF file includes:

Materials and Methods

Fig. S1. Specificity of hRBP3 ELISA, human vitreous IL-6 concentrations, and effects of intravitreal (IVT) injection with rhRBP3 in rats.

Fig. S2. Effects of IVT injection with rhRBP3 on retinal thickness by OCT at 2 months after diabetes in rats.

Fig. S3. Establishment of subretinal overexpression of hRBP3 in rats and effects of diabetes on degradation of RBP3 in rat retina.

Fig. S4. Establishment of Tg mice with hRBP3 overexpression in retina.

Fig. S5. Effects of hRBP3 on VEGF- and FGF-induced migration.

Fig. S6. Effects of rhRBP3 on HG induced *Vegf* and *Il-6* mRNA expression.

Fig. S7. Glucose transporter gene expressions and effects of rhRBP3 on 3-O-MG and 2DG uptake.

Fig. S8. Effects of human vitreous or different peptide of hRBP3 on 2DG uptake, VEGF-induced pTyr-VEGFR2, and palmitate-induced OCR.

Fig. S9. Human vitreous RBP3 concentrations and HbA1c.

Fig. S10. Effects of rhRBP3 or Medalist patient vitreous from protected eye on endothelial migration.

Table S1. Clinical and demographic characteristics by disease status for Medalist patients included in proteomic analysis by mass spectroscopy.

Table S2. Four candidates of up-regulated proteins selected by proteomic analysis in retina and vitreous of Medalist patients with no-mild NPDR ($n = 6$, protected) versus PDR ($n = 11$, nonprotected).

Table S3. RBP3 protein was selected from among the four candidates in table S2.

Table S4. Clinical and demographic characteristics by disease status for individuals included in proteomics and ELISA assays.

Table S5. Up-regulated proteins in the retina from Joslin Medalist patients: protected versus nonprotected.

Table S6. Up-regulated proteins in the vitreous from Joslin Medalist patients: protected versus nonprotected.

Table S7. Primers sequences used in reverse transcription polymerase chain reaction.

References (30–40)

Other Supplementary Material for this manuscript includes the following:

(available at stm.sciencemag.org/cgi/content/full/11/499/eaau6627/DC1)

Table S8. Raw data (Excel file).

Data file S1 (Microsoft Word file). Full immunoblot and silver staining.

Materials and Methods

Proteomic analysis. Post-mortem ocular globes from medalist patients were procured ≈ 10 hours after death and shipped on ice. Approximately 1-1.5 cc of vitreous and retina were extracted from each eye and frozen at -80°C . Retinal lysate (120 μg) and vitreous (20 μl) was separated by 10% SDS-PAGE, stained with Coomassie Blue and analyzed by LC-MS/MS using a linear ion-trap mass spectrometer as described before (28). Complete proteomic peptide hits are included in tables S5 and S6.

Collection of validation specimens. RBP3 was quantified in the vitreous from 54 medalist patients and other diabetic patients with type 1 and 2 diabetes. This group consists of non-diabetic controls (NDM, n [participants]=13), no-mild nonproliferative DR (no-mild NPDR, $n=19$), moderate NPDR ($n=8$) and PDR ($n=14$). DR status was assessed in non-medalist patients by clinical examinations as reported by medical record (8). PDR includes some patients with the history of treatment with laser photocoagulation. RBP3 concentrations in the vitreous were determined by specific ELISA for RBP3 as described above. Vitreous VEGF concentrations were measured by ELISA (R&D systems) in a subgroup of 43 of these individuals (NDM, n [participants]=9; no-mild NPDR, $n=15$; moderate NPDR, $n=7$ and PDR, $n=12$) who had adequate volume of vitreous for the assay. Vitreous IL-6 concentrations were measured by ELISA (R&D systems) in a subgroup of 12 of these individuals (NPDR, $n=6$; PDR, $n=6$). For the detection of degradation of vitreous RBP3, bands (<135 kDa) /all RBP3 bands were assessed by immunoblot in the vitreous from

74 medalist patients and other diabetic patients with type 1 and 2 diabetes. This group consists of NDM (n=12), no-mild NPDR (n=25), moderate NPDR (n=11), PDR (n=26).

Establishment of transgenic mice with human RBP3 overexpression in retina. We

generated RBP3 transgenic (RBP3Tg) mice that specifically overexpressed human RBP3 to the retina (RhRBP3 Tg) using the rhodopsin promoter on a C57BL/6J background. RBP3 transgenic mice, which overexpress human RBP3 (hRBP3) was cloned into the pRho-DsRed vector (Addgene) (pRho-RBP3-Myc-T2A-DsRed) after digested with EcoRI and MluI (New England BioLabs) and driven by the mouse rhodopsin promoter. The pRho-RBP3-Myc-T2A-DsRed was microinjected into embryo of C57BL/6J as background in the Transgenic Core at Brigham and Women's Hospital. Founders were screened by genotyping with PCR using a forward primer (5'-AATAACGCCCCCAATCTCCG-3') and a reverse primer (5'-GATCGTTCAGGGAGCTCTGC-3'). The PCR conditions were 94°C for 3 minutes, followed by 35 cycles of 94°C for 30 seconds, 57°C for 30 seconds, and 72°C for 30 seconds. After 2 months of diabetes induced by STZ, retinal mRNA and protein expressions of RBP3 and VEGF (Mouse VEGF Quantikine ELISA, cat. # MMV00, R&D systems), retinal mRNA expressions of IL-6 as well as analysis of retinal functions by ERG, structures by OCT, and RVP were assessed. Retinal vascular pathology was assessed at six months after STZ injection by identification of acellular capillaries per square millimeter of retinal area.

Establishment of Specific ELISA for RBP3. Nunc ELISA/EIA 96 well plates (Thermo Fisher Scientific) were coated with a 100 μ l of polyclonal RBP3 antibody in filtered PBS (4 μ g/mL/well, ProteinTech) and incubated overnight at room temperature (RT). Plates were washed 3 times with 400 μ l/well of washing buffer including 0.05% Tween-20 and 0.01% SDS and blocked with 300 μ l/well of dilution buffer containing 5% of Tween-20 for 30 minutes at 37°C. Duplicates of 100 μ l of serially diluted rhRBP3 peptides (Origene) as a standard, human vitreous samples (1/10 dilution) and the same amount concentration of IgG (1 μ g/mL), albumin (1 μ g/mL) and RBP4 peptides (1 μ g/mL) as a negative control were loaded on the same plate. After 1 hour incubation at 37°C, the plates were washed 5 times with 400 μ l/well of washing buffer and incubated with 100 μ l of biotinylated monoclonal RBP3 antibody (2 μ g/mL/well, Sigma-Aldrich) for 1 hour at 37°C. Plates were washed 5 times with 400 μ l of washing buffer and incubated with 100 μ l of Streptavidin-HRP (1:200, R&D systems) for 30 minutes at 37°C. After 30 minutes incubation at 37°C, the plates were washed and incubated with 100 μ l/well of TMB for 10-20 minutes at RT. The reaction was stopped with 50 μ l of 1 M H₂SO₄ and absorbance was read at 450 nm using a Plate Reader (Promega).

Reagents. Heparin (cat. # H3149), bovine serum albumin (BSA, cat. # A7888), Streptozotocin (STZ), and Cytochalasin B (cat. # C2743), rotenone (cat. # R8875), and antimycin A (cat. # A8674) were purchased from Sigma-Aldrich. Endothelial cell growth

supplement (ECGS, cat. # J64516) was purchased from Roche Applied Science. RIPA buffer (cat. # BP-115) was purchased from Boston Bioproducts. Protease inhibitor (cat. # 11836153001) was purchased from Roche Diagnostics. Phosphatase inhibitor (cat. # 78420) was purchased from Thermo Scientific. STF31 (cat. # sc-364692) was purchased from Santa Cruz Biotechnology. Antibodies used for specific ELISA assay for RBP3 were: polyclonal RBP3 antibody as a capture antibody was purchased from ProteinTech (cat. # 14352-1-AP); monoclonal RBP3 antibody as a detection antibody was purchased from Sigma-Aldrich (cat. # WH0005949M1). Antibodies used for immunoprecipitation were: VEGFR2 antibody (cat. # sc-504) was purchased from Santa Cruz Biotechnology; Anti-RBP3 antibody (cat. # 14352-1-AP) was from Proteintech; Anti-GLUT1 antibody (cat. # NB300-666) was from Novus Biologicals. Antibodies used for immunoblots are as follows: Anti-RBP3 antibodies were from Abcam (cat. # ab101456), from Proteintech (cat. # 14352-1-AP) and from Sigma-Aldrich (cat. # WH0005949M1); Phospho-tyrosine antibody (cat. # 05-321) was from Millipore; VEGFR2 antibody (cat. # 05-554) was from Upstate; Anti-GLUT1 antibody (cat. # NB300-666) was from Novus Biologicals. Anti-Myc-Tag (cat. # 2272) were from Cell Signaling Technology. Anti-human retinol-binding protein antibody (cat. # A0040) was from Dako. VEGF (cat. # sc-152) and HRP-conjugated anti- β -Actin (cat. # sc-47778) were purchased from Santa Cruz. Recombinant human protein are as follows: recombinant human RBP3 protein (rhRBP3, cat. # TP603816) from human HEK293 cells was obtained from

Origene Technologies. Recombinant human VEGF 165 (rhVEGF, cat. # 293-VE-010) and recombinant human RBP4 protein (rhRBP4, cat. # 3378-LC) were purchased from R&D Systems. Different peptides of RBP3 were: rhRBP3 (aa19-320, 34 kDa, D1, cat. # LS-G12036) was obtained from LSBio, Inc and rhRBP3 (aa321-630, 35 kDa, D2, cat. #ab215617) was obtained from Abcam.

Cell cultures. Cells were maintained at 37 °C in a humidified atmosphere of 5% CO₂.

Bovine retinal endothelial cells (BRECs) and bovine aortic endothelial cells (BAECs).

Primary cultures of BREC and BAEC were isolated as reported previously (30). BREC and BAEC were grown in DMEM with 10% horse serum, 100 µg/ml heparin and 50 µg/ml endothelial cell growth supplement on 0.2% gelatin-coated dishes. We used cells from passages 3 through 6. Serum free DMEM with 0.1% BSA was used for overnight starvation.

Müller cell. Müller cell (cat. # ENW001, Kerfast) were cultured in DMEM containing 10% Fetal Bovine Serum (FBS) and 1% penicillin/streptomycin.

Y79 cell. Y79 human retinoblastoma cells (cat. # HTB-18, ATCC) were grown in RPMI-1640 medium supplemented with 10% FBS and 1% penicillin/streptomycin. Y79 cells were seeded in plates previously coated with poly-L-Lysine (cat. #0403, Sciencell, ScienCell Research Lab.) for experiments.

RPE cell. Human retinal pigmented epithelium (RPE) cells (cat. #6540, ScienCell Research Lab.) were maintained in epithelial cell medium (EpiCM, cat. #4101, ScienCell Research

Lab.) supplemented with 10 % FBS, 1x epithelial cell growth supplement (EpiCGS, cat. #4101, ScienCell Research Lab.) and 1% penicillin/streptomycin. Cells were seeded in plates previously coated with poly-L-Lysine (cat. #0403, ScienCell Research Lab.) for experiments

C2C12 myoblast. C2C12 myoblasts (ATCC) were cultured in DMEM containing 10% FBS, 25 mM glucose (HG) and 1% penicillin/streptomycin for proliferation. Differentiation was induced by incubating the cells in DMEM containing 2% horse serum, HG and 1% penicillin/streptomycin for 8 days.

WT-1 cell. Immortalized brown preadipocytes (WT-1) were cultured in DMEM containing HG supplemented with GlutaMAX 10% FBS. For adipogenic induction, WT-1 cells were seeded at a density of 1×10^5 cells/cm². Two days later when cells were fully confluent, cells were then exposed to an induction cocktail for two days, which consisted of 0.5 mM of 3-isobutyl-1-methylxanthine (IBMX), 125 μ M of indomethacin, 5 μ M of dexamethasone, 20 nM of insulin and 1 nM of T3 in HG DMEM, followed by a six-day maintenance phase (DMEM containing HG, 20 nM of insulin and 1 nM of T3).

Cell-based assays. Purity of recombinant human RBP3 protein (rhRBP3), obtained from Origene Technologies, was determined by Coomassie blue staining and SDS-PAGE gel. Scratch assay assessed migration, as published (31). Cells were grown to confluence on 0.2% gelatin-coated 35 mm plates in growth media. Confluent cells were starved in DMEM/0.1%

BSA overnight. Scratch wounds were created in confluent monolayers using a sterile p200 pipette tip. Perpendicular marks were placed at intervals of 1 mm across each scratch on the external surface of the well. After the suspended cells were washed, the wounded monolayers were incubated in each conditions of test medium in DMEM/0.1% BSA media. Osmotic pressure was adjusted in low glucose conditions by adding 19.4 mM mannitol. Every 6 hours up to 24 hours, repopulation of the wounded areas was observed under phase-contrast microscopy (Olympus). Using the NIH ImageJ image processing program, the size of the denuded area was determined at each time point from digital images. The percentage of migration area was calculated as the ratio of covered area (original wound area - open wound area) to the original wound area. Effects of rhRBP3 (0.25 µg/mL) or medalist patient vitreous with high RBP3 expression from protected eyes on high glucose (25 mM glucose, HG)- or VEGF (2.5 ng/mL)-induced endothelial migration were measured in BRECs. Anti-RBP3 antibody was added as a neutralizing antibody (1 µg/mL). 17.2 mg/mL of BSA was added in the group of BSA, VEGF+BSA and Anti-RBP3+BSA while 8.6 mg/mL of BSA was added in the group of Vitreous+BSA, VEGF+Vitreous+BSA and VEGF+Vitreous+Anti-RBP3+BSA.

The effects of hRBP3 on tyrosine phosphorylation and protein expression of VEGFR2 (Flk) in BREC were assessed by immunoprecipitation (IP) with a VEGFR2 antibody (cat. # sc-504, Santa Cruz Biotechnology) followed by immunoblotting (IB) with a phospho-tyrosine antibody (cat. # 05-321, Millipore) or VEGFR2 antibody (cat. # 05-554, Millipore) as

previously described (32). Cells were incubated with vehicle, rhVEGF, rhRBP3, both of rhVEGF and rhRBP3 for 10 minutes after overnight starvation in DMEM with 0.1% BSA. Both of rhVEGF and rhRBP3 were kept at RT for 10 minutes respectively, and then cells were incubated at the same time (Co-addition). Both of rhVEGF and rhRBP3 were premixed at RT for 10 minutes, and then cells were incubated (Pre-incubation). Then, cells were washed with ice-cold PBS and lysed immediately with RIPA buffer including protease inhibitor and phosphatase inhibitor. Cell lysates were immunoprecipitated (IP) with a VEGFR2 antibody followed by immunoblotting (IB). Ratio of tyrosine phosphorylation to total VEGFR2 was quantified by immunoblot and shown as fold-change to basal condition.

Reverse transcription and quantitative real-time PCR analysis. Total RNA was extracted from the retina and cells using RNeasy mini kit (Qiagen), and cDNA was synthesized as previously described (33). All mRNA expressions were normalized to 18S and quantified using the threshold cycle method (34). PCR primers used in the study are listed in table S7.

Immunoblotting. The immunoblot analysis was described previously (35). Briefly, retina lysates or cell lysates were loaded on an SDS-PAGE gel and electroblotted onto a nitrocellulose membrane. After blocking, the membranes were incubated with antibodies. Degradation of RBP3 was calculated as bands <135kDa / all RBP3 bands in each blot. The quantifications of western blotting were performed using ImageJ. Uncropped western gels are shown in Datafile S1.

High glucose (HG) effects in Müller cell. LG or HG was added in Müller cell with rhRBP3 (0, 0.5, 2.5 µg/mL) for 24 hours in DMEM with 3%FBS. 10 µM of STF31 was added as a GLUT1 inhibitor. 100 nM of PMA was added for 3 hours.

Crosslinking. Müller cells were incubated with BSA, boiled rhRBP3, and rhRBP3 for 1 hour at 37 °C, followed by the addition with 2 mM of DTSSP crosslinker (cat. # 21578, Fisher) for 2 hours or Formaldehyde for 30 minutes at 4 °C. After subcellular fractionation (cat. # 78840, Fisher), isolated membrane was immunoprecipitated (IP) with GLUT1 antibody (cat. # NB300-666, Novus Biologicals) or RBP3 antibody (cat. # 14352-1-AP, Proteintech), then immunoblot (IB) was performed.

BRECs were incubated with RBP4, RBP3, and PBS for 1h in 0.2%BSA+DMEM-LG after a 16 hour starvation with 0.2%BSA+DMEM-LG, followed by washing by PBS, then rhVEGF (2.5 ng/mL) was added for 10min in 0.2%BSA+DMEM-LG. Cells were washed by PBS, followed by the addition with 2mM of DTSSP for 2h at 4 °C. Cell lysates were IP with VEGFR2 antibody, then IB was performed.

Silver staining. After electrophoresis of the proteins in the polyacrylamide gel, silver staining is performed by silver stain kit (cat. # PROT-SIL2, Sigma-Aldrich) according to manufacturer's instructions.

Radioactive materials.

3-*O*-[³H]methyl-D-glucose ([³H]3-*O*-MG, cat. #NET379001MC) and

2-deoxy-D-1- ^3H glucose (^3H 2DG, cat. #NET328A001MC) were obtained from PerkinElmer.

Measurement of 3-O-MG uptake. The cells were rinsed 5 times with PBS and incubated with the assay medium (0.1% BSA+PBS+1 mM of CaCl_2 and 2.5 mM of MgSO_4) containing rhRBP3 (0, 0.25 $\mu\text{g}/\text{mL}$) for 1 hour at 37 °C, and incubated with 0.1 mM of 3-O-MG, 2 μCi of ^3H 3-O-MG for 1 minute at RT. Noncarrier-mediated uptake was determined in incubations containing 10 μM of cytochalasin-B for 5 minutes. The uptake was terminated by the addition of 50 μM of cytochalasin-B for 30 seconds, followed by 5 washes with ice-cold PBS. After washes, cell associated radioactivity was solubilized in 50 mM of NaOH, and taken for liquid scintillation counting. Results shown are corrected for total cellular protein content, as assessed by the bicinchoninic acid (BCA) assay (ThermoFisher Scientific).

Measurement of 2DG uptake. The cells were rinsed and incubated with the assay medium as described above containing several concentrations of rhRBP3 for 1 hour at 37 °C, and then incubated with 0.1 mM of 2DG, 1 μCi of ^3H 2DG for 5 minutes at RT. Noncarrier-mediated uptake was determined in incubations containing 10 μM of cytochalasin-B for 5 minutes. 10 μM of STF31 (cat. # sc-364692, Santa Cruz Biotechnology) was used as a GLUT1 inhibitor for 5 minutes. Anti-RBP3 antibody was added as a neutralizing antibody (1 $\mu\text{g}/\text{mL}$). The uptake was terminated by 5 washes with ice-cold PBS. After washes, the cells were processed for liquid scintillation counting. Results shown are corrected for total cellular protein content

as described above.

Measurement of 2DG uptake with different fragment of RBP3. Different molecular sizes of RBP3 such as rhRBP3 (aa19-320, 34 kDa, D1, cat. # LS-G12036, LSBio, Inc) and rhRBP3 (aa321-630, 35 kDa, D2, cat. #ab215617, Abcam) were used. Müller cells were rinsed and incubated with 40 nM of rhRBP4 (RBP4, 22 kDa, cat. #3378-LC, R&D Systems), 40 nM of full length of rhRBP3 (full, 135 kDa, cat. # TP603816, Origene Technologies), and 40 nM of different peptides of rhRBP3 (D1, D2, and combination with D1 and D2) for 1 hour at 37 °C after a 4 hour starvation with 0.2% BSA+DMEM-L, and then incubated with 0.1 mM of 2DG, 1 µCi of [³H]2DG for 5 minutes at RT. 10 µM of STF31 was used as a GLUT1 inhibitor for 5 minutes. [³H]2DG uptake was terminated by 5 washes with ice-cold PBS. After washes, the cells were processed for liquid scintillation counting. Results were corrected for total cellular protein content as described above.

Extracellular acidification rate (ECAR). All ECAR were measured by a Seahorse XFe96 Flux Analyzer (Agilent Technologies). In vitro study, Müller cells were seeded into a 96-well plate 1 day before measurement. Cells were incubated with vehicle, boiled rhRBP3 (b-RBP3), or rhRBP3 (RBP3) for 1 hour in assay medium (0.2% BSA+KRB buffer: 110 mM of NaCl, 4.7 mM of KCL, 2 mM of MgSO₄, 1.2 mM of Na₂HPO₄, and 0.24 mM of MgCL₂, pH7.4) before measurement. For ex vivo study, whole retinas were isolated from mice after 4 months duration of diabetes. One fourth of the retina was loaded into the 96-well plate and was

incubated in the assay medium for 1 hour before measurements. No glucose was included in the assay medium. Data are calculated after the addition of LG, HG, rotenone (0.5 μM or 2.0 μM) and antimycin A (0.5 μM or 2.0 μM), 2DG (50 mM or 100 mM) for Müller cell or retina, respectively, and corrected for total protein content measured by BCA assay. For each experiment, the means from 2- 4 replicate wells were recorded.

In vivo study. Insulin deficient diabetic rats were produced by intraperitoneal injection of streptozotocin (STZ, 55 mg/kg) after a 12 hours overnight fast at 6 weeks of age and insulin deficient diabetic mice were produced by 5 consecutive days of intraperitoneal injection of STZ (50 mg/kg) at 7 weeks of age. Diabetes is ascertained by blood glucose values > 250 mg/dl as measured by a glucometer and followed at 3-4 week intervals (36, 37). The experimental protocols were approved by the Joslin Diabetes Center Institutional Animal Care and Use Committee. The experiments were carried out in strict accordance with the recommendations in the Guide for the Care and Use of Laboratory Animals of the National Institutes of Health.

In vivo intravitreal (IVT) injection. IVT injections were performed by injecting 5 μL volumes via a 32G Hamilton syringe (Hamilton Corp.) at 2 mm below the limbus of male Lewis rats at 8 weeks of age (Charles River Laboratories, Inc.), as described previously (38). In the premix study, recombinant human VEGF (rhVEGF, 200 ng/mL) and rhRBP3 (2.5 $\mu\text{g/ml}$, 20 nM) were combined and immediately injected into the vitreous. Each rat was

infused with Evans blue dye 10 minutes after IVT injection, and 2 hours later retinal vascular permeability (RVP) was assessed (36). In an intervention study, IVT of rhVEGF (200 ng/mL) was followed 24 hours later by an IVT of vehicle, boiled rhRBP3 (2.5 µg/ml, 20 nM), or rhRBP3 (2.5 µg/ml, 20 nM). In dose dependent of rhRBP3 study, IVT of rhVEGF (200 ng/mL) was followed 24 hours later by an IVT of vehicle or rhRBP3 (1, 10, 20 nM). At 10 minutes after IVT injection with rhRBP3, each rat was infused with Evans blue dye and 2 hours later RVP was assessed. After 2 months of diabetes, vehicle, boiled rhRBP3, or rhRBP3 were IVT injected (2.5 µg/ml, 20 nM). At 3 days after IVT injection, RVP and retinal mRNA expressions of Vegf and Il-6 and retinal protein expressions of VEGF (Rat VEGF Quantikine ELISA Kit, cat. # RRV00, R&D systems) were assessed. In addition, at 3 days post IVT injection, scotopic responses of the neuroretina to maximal white light flash was measured by dark-adapted electroretinogram (ERG) (ADInstruments). Thickness of the retina and sub-layers were also evaluated by spectral domain optical coherence tomography (SD-OCT 840) and segmentation software Diver v2.4 (Bioptigen) (38). Boiled rhRBP3 was obtained by boiling with 100°C for 30 minutes, and left for 30 minutes at RT.

In vivo gene therapy with human RBP3.

Subretinal overexpression of hRBP3, in male Lewis rats (Charles River Laboratories International, Inc.), was performed using lentiviral vectors expressing RBP3 or luciferase-GFP driven by CMV-promoter (39). We confirmed luciferase expression in rat eyes

at one week, three months and six months after injection using in vivo imaging system (IVIS SPECTRUM CT system; Caliper Life Sciences) with intraperitoneal injection of D-Luciferin Firefly (50 mg/g BW, Caliper Life Sciences). Luciferase-GFP was used to determine efficacy of the vector, which correlated well with the expression of RBP3.

Subretinal injections of lentivirus at the concentrations of luciferase-GFP (OD: 2.5×10^6 IFU) and a cocktail of RBP3/luciferase-GFP (OS: $2.25/0.25 \times 10^6$ IFU) were performed by a trans-corneal method at 2 weeks of age to express hRBP3 and luciferase reporter gene. Differences in luciferase activity between OS and OD were found because different amounts of lentivirus containing luciferase plasmid were injected to track the persistent expression of proteins by sub-retinal injections of lentivirus to assure that each eye has equal amount of virus injected, one retina was injected with both luciferase and RBP3 plasmids in the treated retina and only luciferase plasmid in the untreated retina.

At two months after diabetes, scotopic responses of the neuroretina were measured by ERG, and thickness of the retina and sub-layers were evaluated by OCT (36). Protein expressions of VEGF in retina and vitreous were assessed as described above. RVP was measured using Evans blue dye permeation (36). Retinal vascular pathology was assessed at six months after STZ injection to identify acellular capillaries per square millimeter of retinal area (40).

In Vivo Retinal Assessments.

Optical Coherence Tomography (OCT).

The thickness of the total retina and retinal sub-layers were measured by spectral domain optical coherence tomography (SD-OCT 840) and segmentation software Diver v2.4 (Biotigen) (36).

Electroretinogram (ERG).

Scotopic responses of the neuroretina to maximal white light flash are measured by dark-adapted ERG (ADInstruments) at 2 months after STZ injection (36). The ERG system consists of a light stimulator (WLS-20, Mayo Co.), differential amplifier (Bio Amp), analog to digital convertor (PowerLab/4sp, ADInstruments) and software (Scope for Windows V3.6.4).

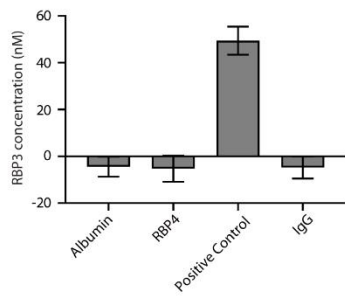
The light source consists of a white light emitting diode, contact lens with embedded gold wire electrode which connects to the stimulator. Prior to each session, the LED lens is calibrated using the WLS-20 light sensor and calibration routine.

At 2 months after STZ injection, rats were dark-adapted within the ERG room overnight. For maximum light flash stimulation, intensity of 1.4×10^4 cd/m² with duration of 5 msec used.

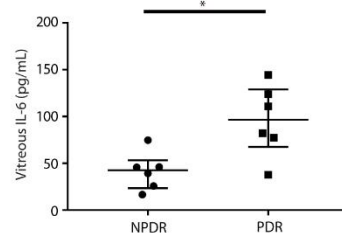
The signals were filtered with a bandpass filter between 1 and 500Hz (PowerLab ML750) to reduce background noise. At least three signals were recorded with an interval of 60 seconds between stimulations. An average of all signals are used in the data analysis. Analysis of the data is performed using the ADInstruments Scope V3.6.4 software.

Figure S1

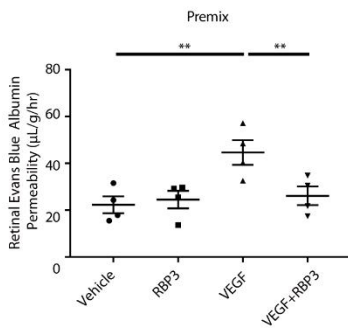
A



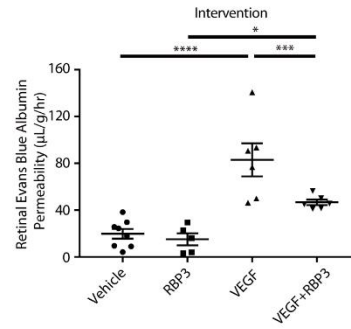
B



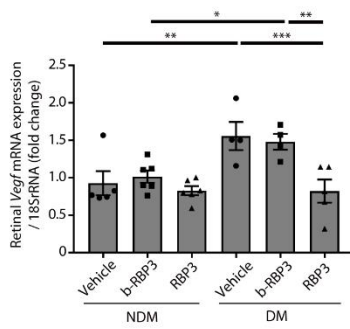
C



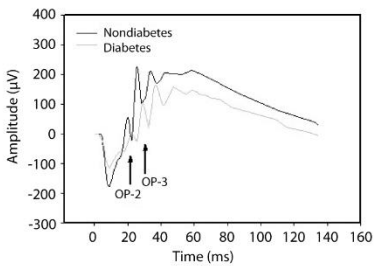
D



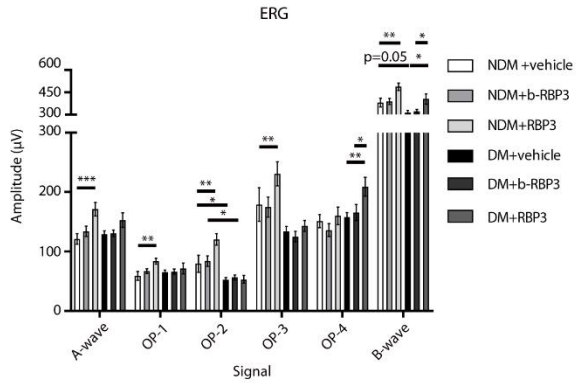
E



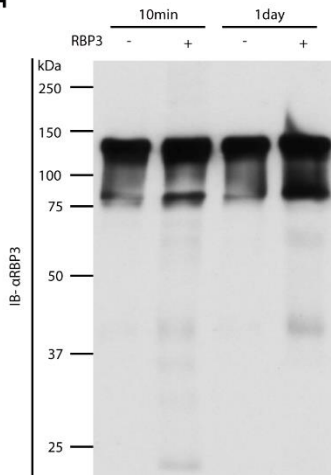
F



G



H



I

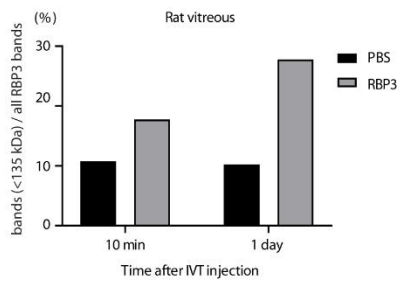
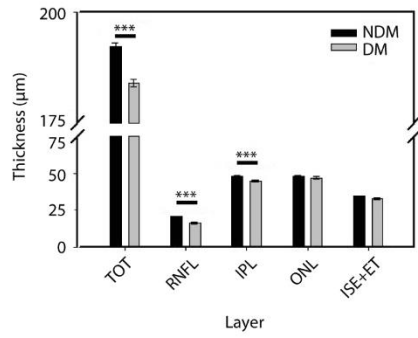


Fig. S1. Specificity of hRBP3 ELISA, human vitreous IL-6 concentrations, and effects of intravitreal (IVT) injection with rhRBP3 in rats.

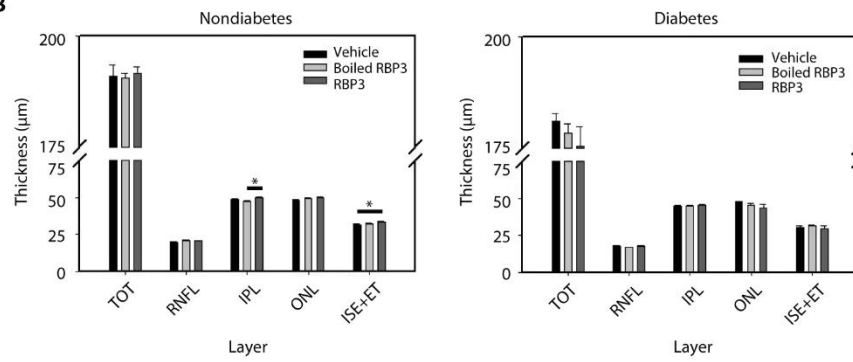
(A) Specific and sensitivity of ELISA for RBP3. Positive control= human vitreous from NPDR. $n = 3$. (B) Human vitreous IL-6 concentrations from NPDR and PDR. $n = 6$. (C) Retinal vascular permeability (RVP) by premixed with recombinant human VEGF (rhVEGF) and rhRBP3. $n = 4$. (D) RVP by intervention in rat. $n = 5-8$. (E) Retinal Vegf mRNA expression at 2 month after STZ injection. $n = 4-6$. (F and G) Electroretinogram (ERG) at 2 month after STZ injection. (F) ERG at baseline. (G) ERG at 3 days after IVT injection. $n = 9-13$. (H and I) Degradation of vitreous RBP3 in rat at 10min and 1 day after IVT injection with rhRBP3 by immunoblot analysis. $n = 1$. NDM = non-diabetic rats. DM = diabetic rats. Vehicle, b-RBP3, and RBP3 = injected with vehicle, boiled rhRBP3 and rhRBP3. $n =$ numbers of eyes. All data are represented as mean \pm SEM. Group comparison was done by ANOVA. When overall F tests were significant ($p < 0.05$), Fisher's LSD test was used to determine the location of any significant pairwise differences. **** $p < 0.0001$, *** $p < 0.001$, ** $p < 0.01$, * $p < 0.05$.

Figure S2

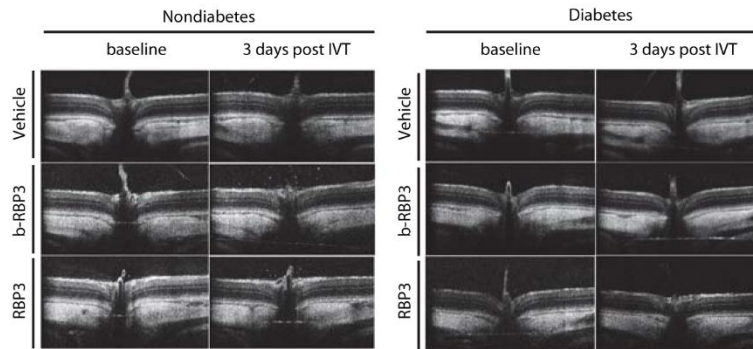
A



B



C



D

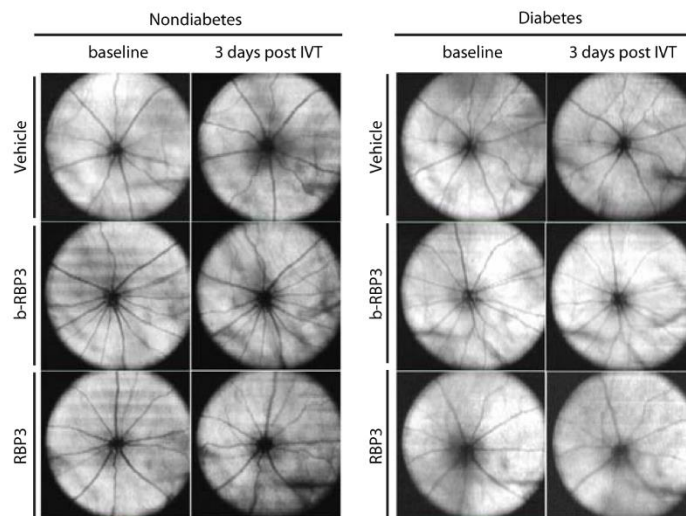


Fig. S2. Effects of IVT injection with rhRBP3 on retinal thickness by OCT at 2 months after diabetes in rats.

(**A**) baseline. NDM, $n = 16$; DM, $n = 21$, (**B**) 3 days after IVT injection. $n = 9-11$. (**C**) OCT-B scan and (**D**) OCT-enface. $n =$ numbers of eyes. NDM = non-diabetic rats. DM = diabetic rats.

Vehicle, b-RBP3, and RBP3 = injected with vehicle, boiled rhRBP3 and rhRBP3. All data are represented as mean \pm SEM. Group comparison was done by ANOVA (same as fig. S1).

Figure S3

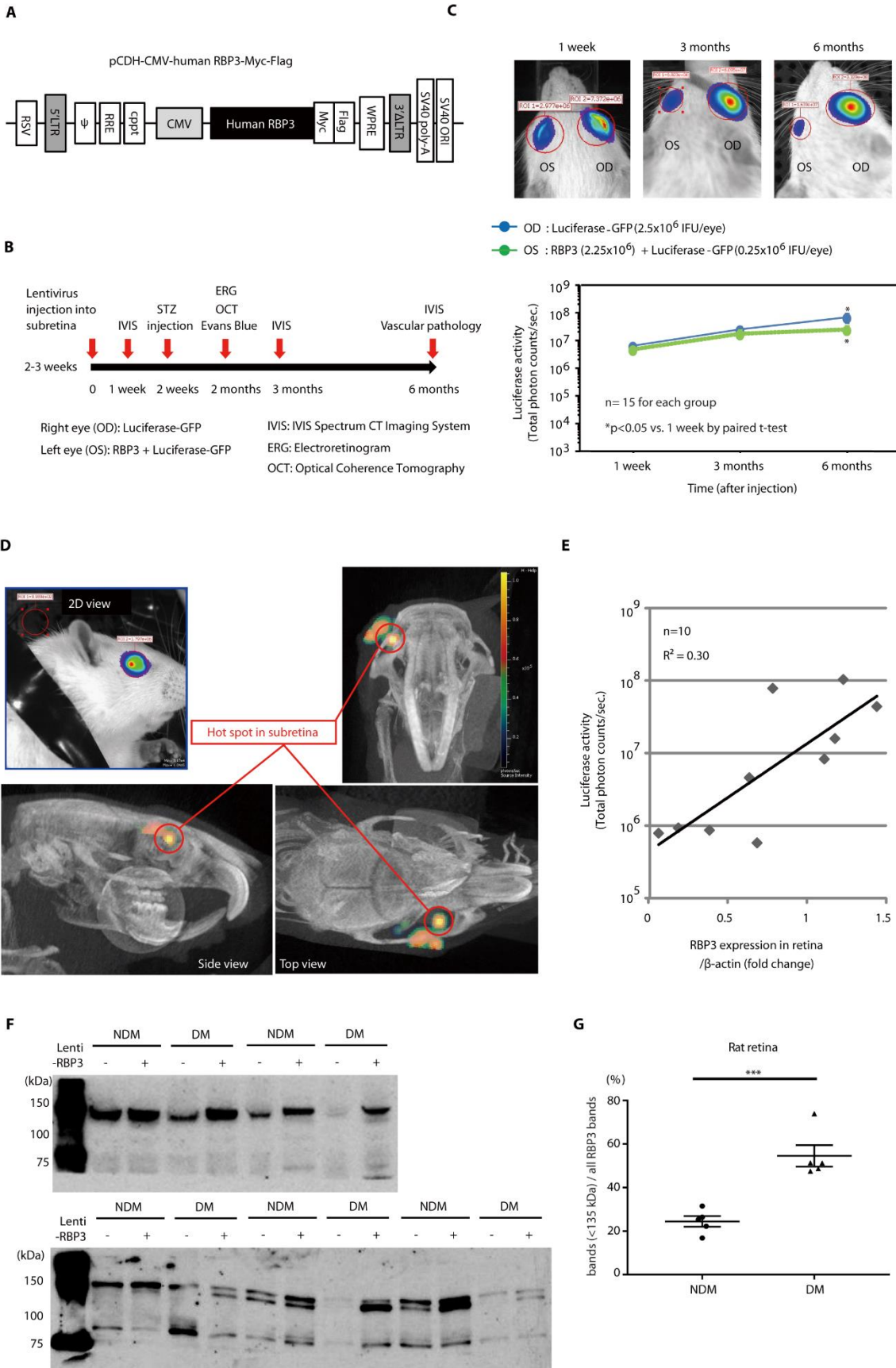


Fig. S3. Establishment of subretinal overexpression of hRBP3 in rats and effects of diabetes on degradation of RBP3 in rat retina.

(A) Lentiviral vector expressing hRBP3 driven by CMV-promoter. (B) Time course of overall in vivo experimental period. (C) Luciferase expression in rat eyes using in vivo imaging system (IVIS Lumina system; Caliper Life Sciences, Hopkinton, MA). OD = 15 eyes, OS = 15 eyes. p-values were calculated by linear mixed effects modeling, comparison by paired t-test were conducted to determine the location of any significant pairwise differences. (D) Co-registered optical and micro CT showing 3D localization of signal. (E) Association of luciferase activity and the expression of RBP3 in retina assessed by linear regression. N = 10 eyes. (F and G) Effects of diabetes on degradation of RBP3 by immunoblot analysis in rat retina. $n = 5$. n = numbers of eyes. NDM = non-diabetic rats. DM = diabetic rats. All data are represented as mean \pm SEM.

Figure S4

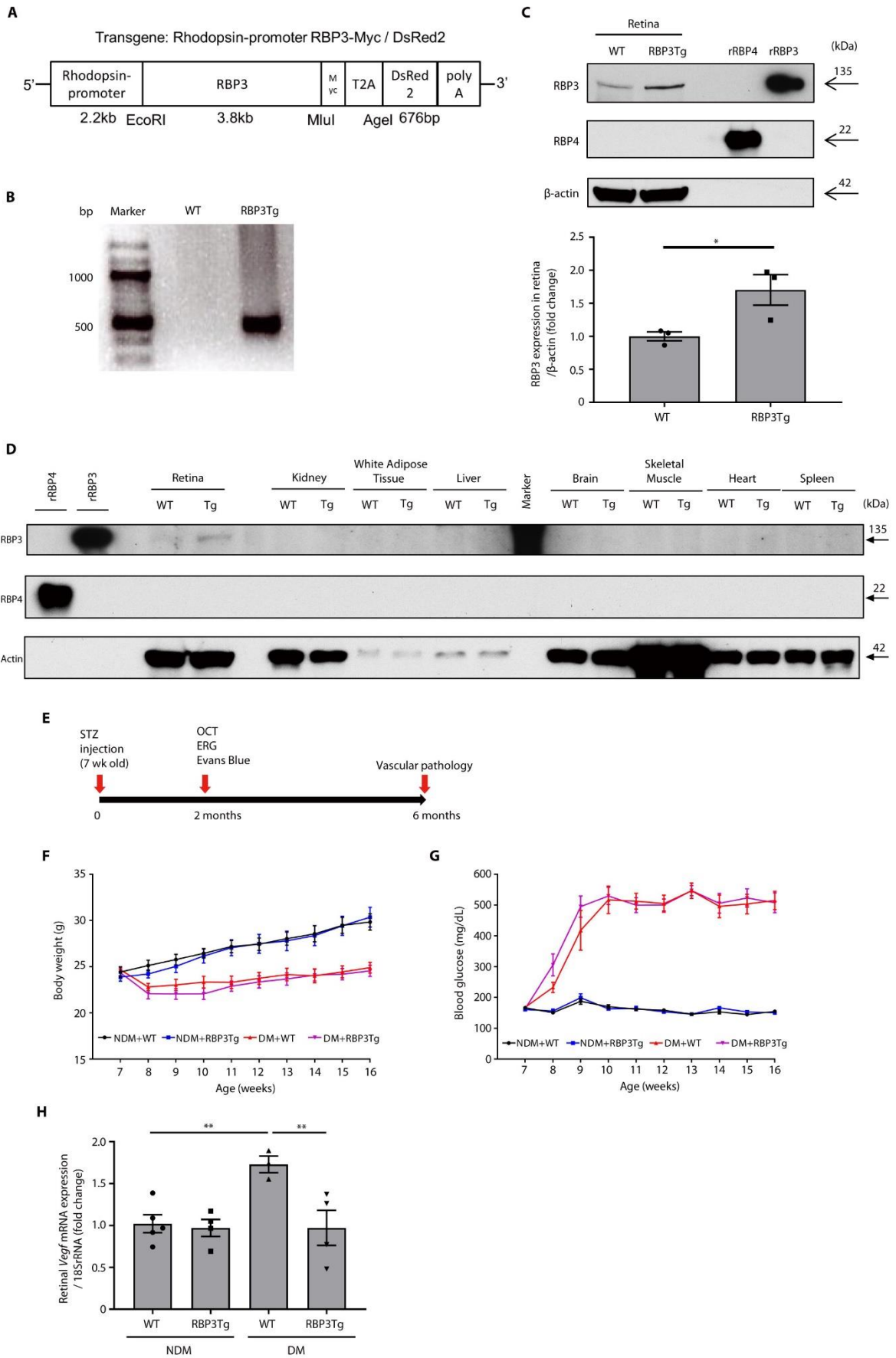
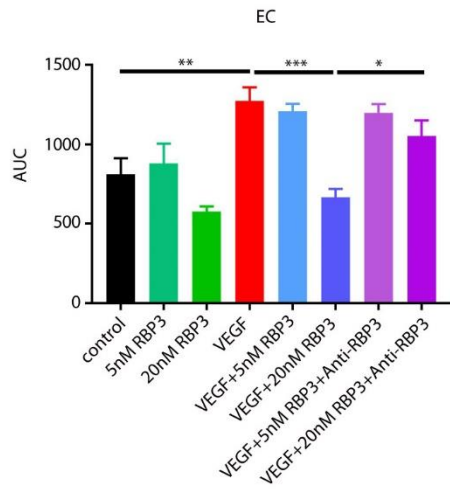


Fig. S4. Establishment of Tg mice with hRBP3 overexpression in retina.

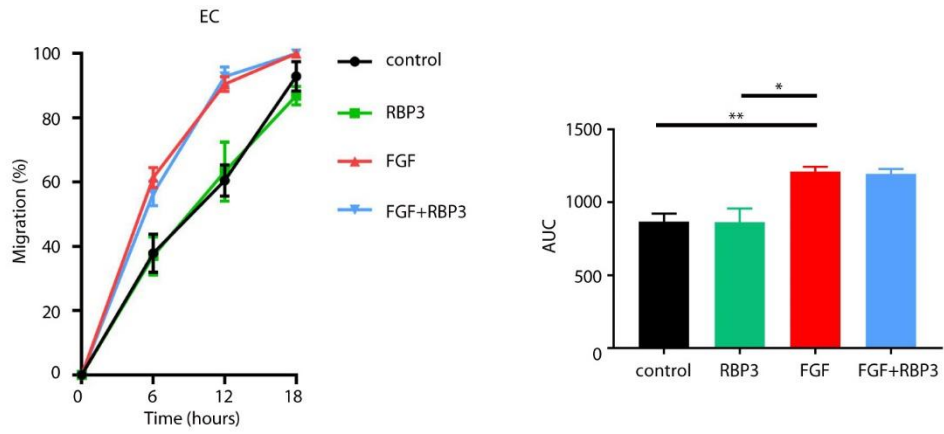
(A) Rhodopsin-promoter derived RBP3 transgene. (B) Genotyping. (C and D) RBP3 expressions in (C) retina, $n = 3$ and (D) several tissues by western blot. rhRBP3 = recombinant human RBP3. rhRBP4 = recombinant human RBP4. (E) Timeline of the in vivo experiment. (F and G) Changes of body weight and blood glucose. $n = 7-10$. (H) Vegf mRNA expression in retina at 2 months after diabetes. $n = 3-5$. WT= wild type mice, RBP3Tg= RBP3 transgenic mice, All data are represented as mean \pm SEM. Group comparison was done by ANOVA (same as fig. S1 and 2).

Figure S5

A



B



C

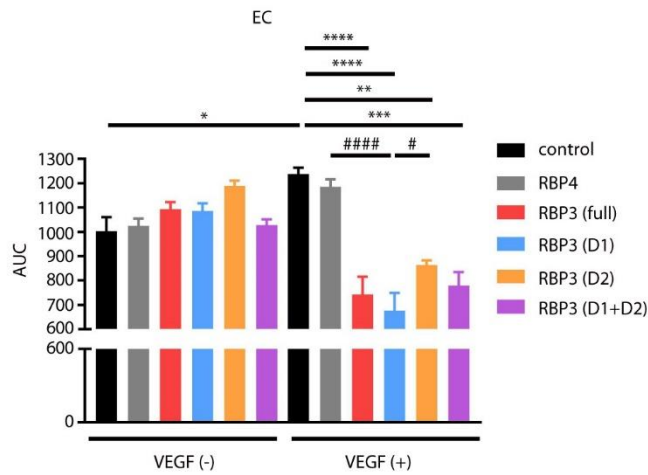
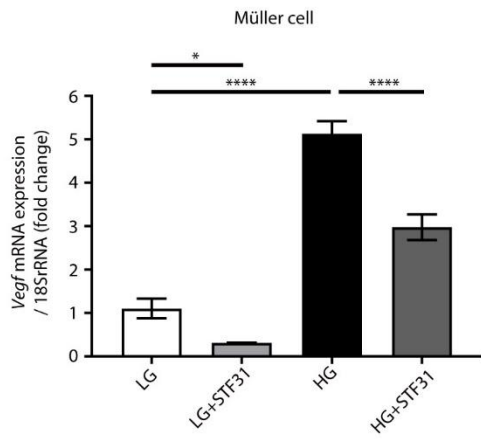


Fig. S5. Effects of hRBP3 on VEGF- and FGF-induced migration.

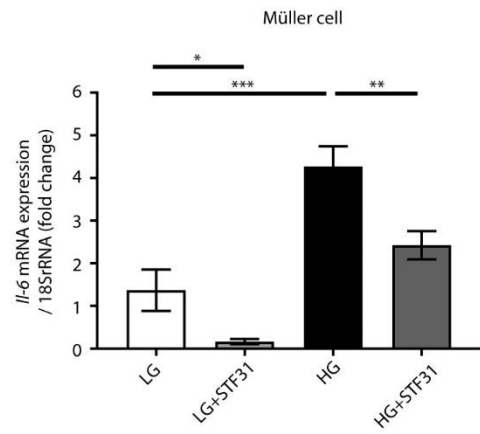
(A) Effects of rhRBP3 (5 nM or 20 nM) on rhVEGF (2.5 ng/mL)-induced endothelial migration in BREC. Area under the curve (AUC) for Fig. 5D. $n = 4$. (B) Effects of rhRBP3 (20 nM) on FGF (10 pg/mL)-induced endothelial migration in BAEC. $n = 3-4$. (C) Effects of RBP4 (20 nM) or different peptide of rhRBP3 (20 nM) on rhVEGF (2.5 ng/mL)-induced endothelial migration in BAEC. AUC for Fig. 5E. full: full length of RBP3. D1: fragment of RBP3 (AA19-320, domain 1). D2: fragment of RBP3 (AA321-630, domain 2). $n = 4$. All data are represented as mean \pm SEM. Group comparison was done by ANOVA (same as fig. S1, S2 and S4). (C) * $p < 0.05$, ** $p < 0.01$, *** $p < 0.001$ and **** $p < 0.0001$ versus VEGF+control; # $p < 0.05$, ## $p < 0.01$, ### $p < 0.001$ and #### $p < 0.0001$ versus VEGF+RBP3 (D1).

Figure S6

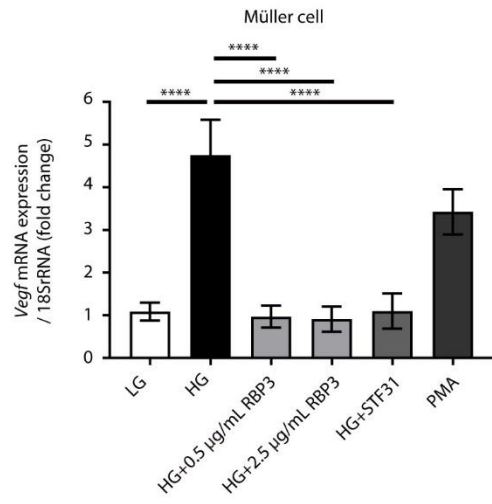
A



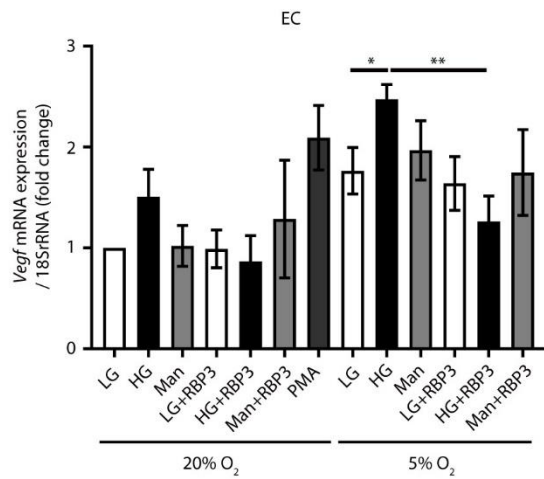
B



C



D



E

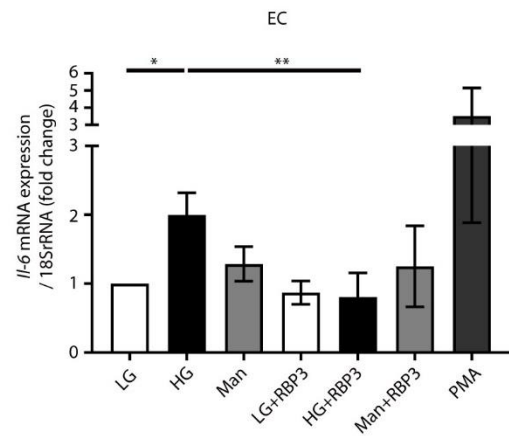


Fig. S6. Effects of rhRBP3 on HG induced *Vegf* and *Il-6* mRNA expression.

(A and B) *Vegf* and *Il-6* mRNA expression in Müller cell. $n = 4$. (C) Effects of rhRBP3 on HG induced *Vegf* mRNA expression in Müller cell. $n = 6$. (D and E) Effects of rhRBP3 on HG induced *Vegf* and *Il-6* mRNA expression in BREC. rhRBP3 (RBP3, 0.25 $\mu\text{g}/\text{mL}$). $n = 4$. LG = 5.6 mM glucose. HG = 25 mM glucose. Man = 25 mM Mannitol. 10 μM STF31 was added as a GLUT1 inhibitor. 100 nM of PMA was added for 3 hours. All data are represented as mean \pm SEM. Group comparison was done by ANOVA (same as fig. S1, S2, S4 and S5).

Figure S7

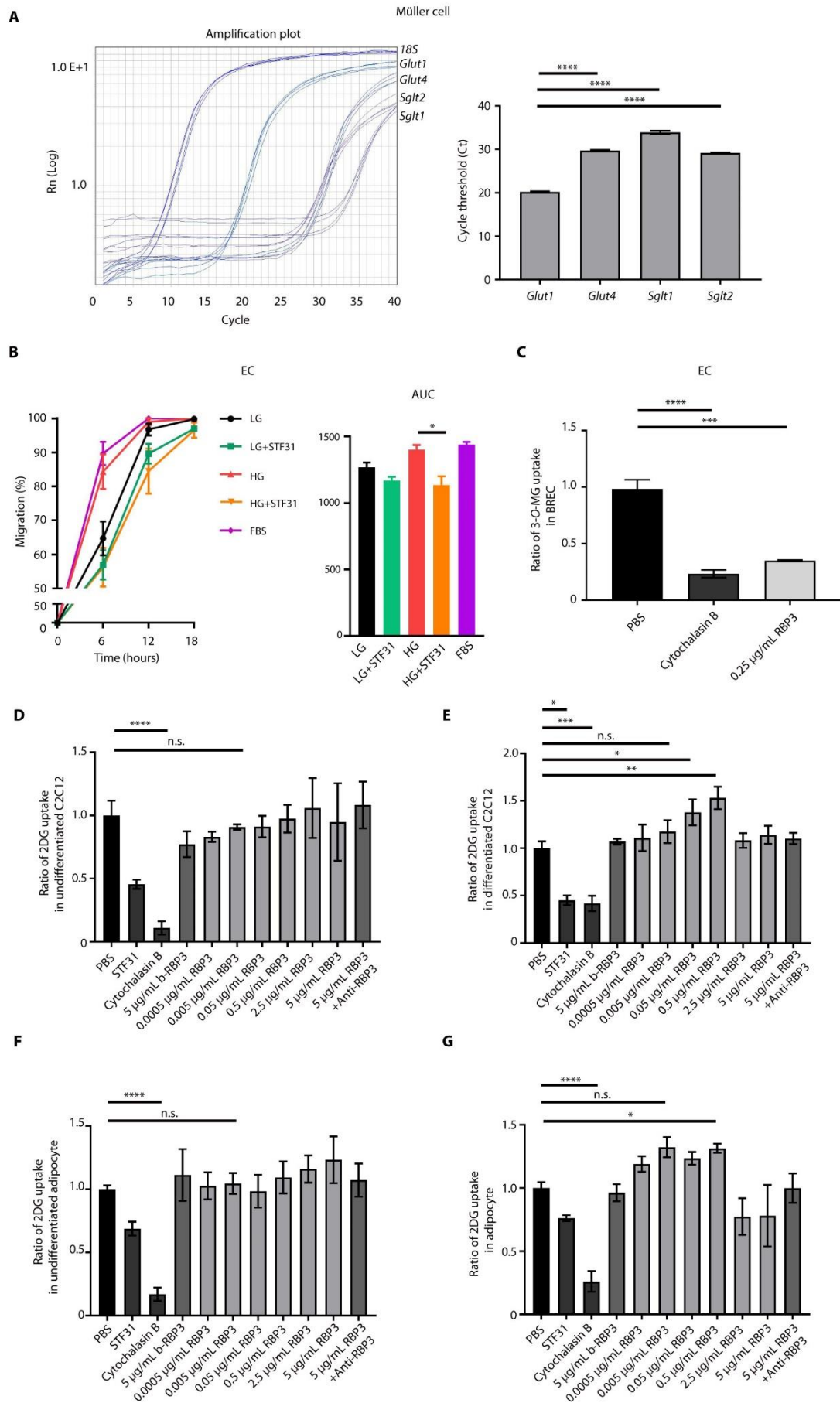


Fig. S7. Glucose transporter gene expressions and effects of rhRBP3 on 3-O-MG and 2DG uptake.

(A) Amplification plot and cycle threshold of potential glucose transporter gene expressions using qRT-PCR in Müller cell. $n = 4$. (B) Effects of STF31, GLUT1 inhibitor (10 μM), on low glucose (LG, 5 mM) or high glucose (HG, 25 mM)-induced migration in BAEC. $n = 3$. (C) Effects of rhRBP3 on 3-O-MG uptake in BREC. $n = 3$. (D to G) Effects of rhRBP3 on 2DG uptake; (D) Undifferentiated C2C12. $n = 3-7$; STF31 ($n = 2$). (E) Differentiated C2C12. $n = 3-7$; STF31 ($n = 2$). (F) Undifferentiated adipocyte. $n = 3-6$. (G) Differentiated adipocyte. $n = 3-6$; STF31 ($n = 2$). b-RBP3 = boiled RBP3. All data are represented as mean \pm SEM. Group comparison was done by ANOVA (same as fig. S1, S2 and S4-S6). (A) **** $p < 0.0001$ versus *Glut1*. (B) * $p < 0.05$ HG versus HG+STF31. (C-G) * $p < 0.05$, ** $p < 0.01$, *** $p < 0.001$ and **** $p < 0.0001$ versus PBS.

Figure S8

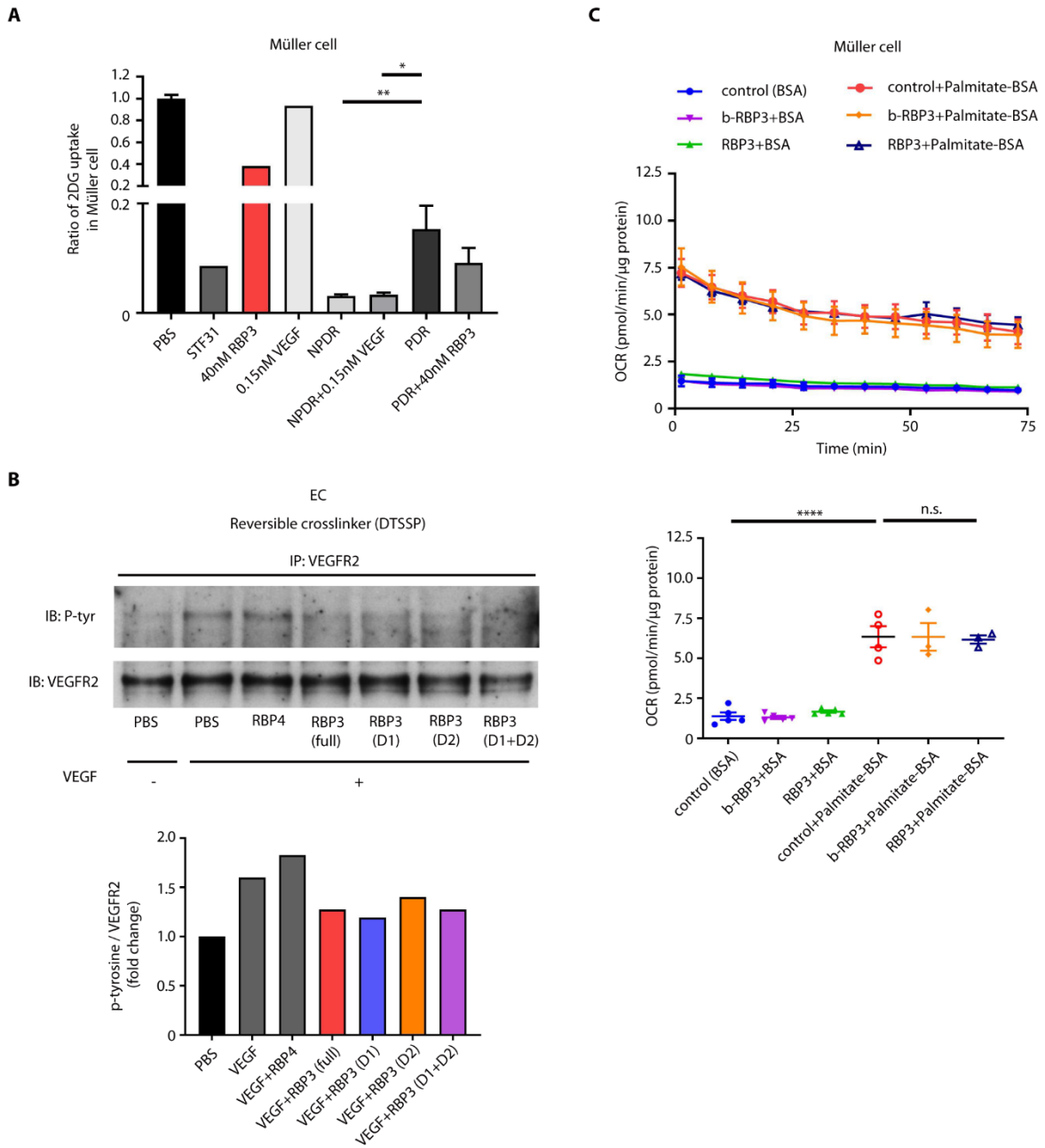


Fig. S8. Effects of human vitreous or different peptide of hRBP3 on 2DG uptake, VEGF-induced pTyr-VEGFR2, and palmitate-induced OCR.

(A) Effects of rhRBP3 (5 μ g/mL, 40 nM) or human vitreous from NPDR (RBP3; 15.7 ± 2.2 nM, VEGF; 8.6 ± 1.6 pM), PDR (RBP3; 5.0 ± 0.6 nM, VEGF; 196.1 ± 69.2 pM) on 2DG uptake in Müller cell. T-test was used to evaluate the difference between NPDR and PDR. $n =$

3. **(B)** Effects of RBP4 (20 nM) or different peptide of rhRBP3 (20 nM) on VEGF (2.5 ng/mL)-induced tyrosine phosphorylation (p-tyrosine) of VEGFR2 in BAEC. full: full length of RBP3. D1: fragment of RBP3 (AA19-320, domain 1). D2: fragment of RBP3 (AA321-630, domain 2). $n = 1$. **(C)** Effects of rhRBP3 on palmitate-induced oxygen consumption ratio (OCR) in Müller cell. Cells were incubated with PBS, boiled rhRBP3 (b-RBP3), rhRBP3 (2.5 μ g/mL, 20 nM) for 1 hour in 0.2%BSA+KRB buffer (no glucose). 200 μ M of BSA or Palmitate-BSA was added to start seahorse assay. $n = 4-6$. All data are represented as mean \pm SEM. Group comparison was done by ANOVA (same as fig. S1, S2 and S4-S7).

Figure S9

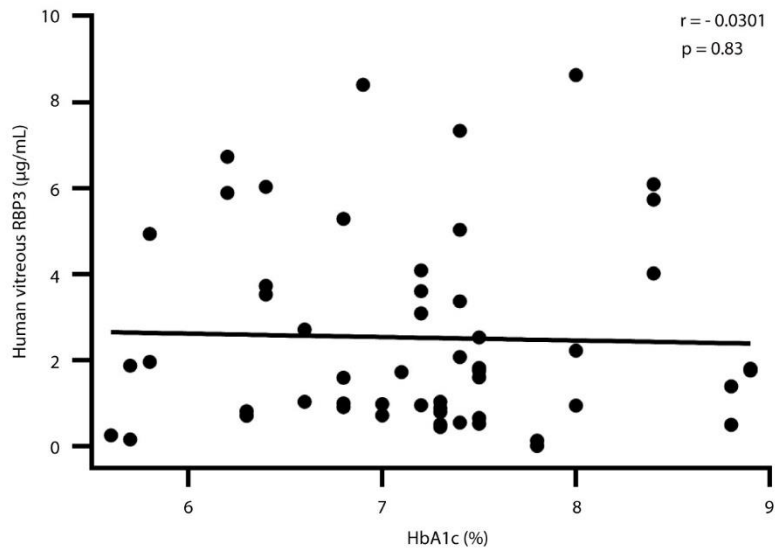
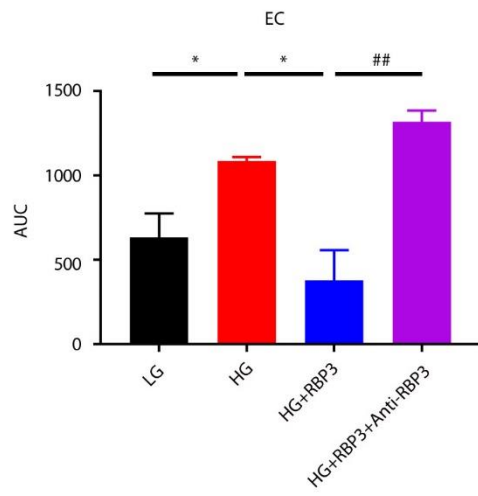


Fig. S9. Human vitreous RBP3 concentrations and HbA1c.

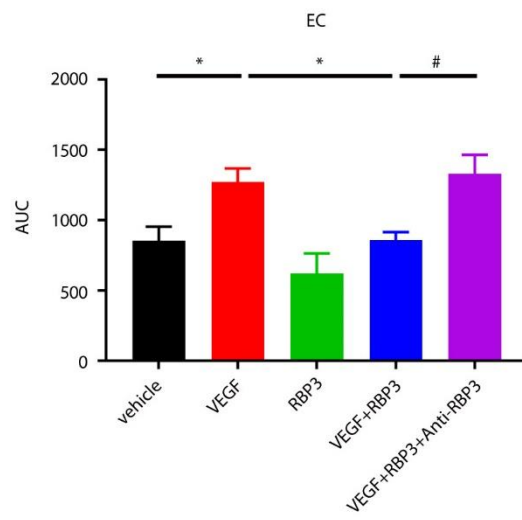
The correlation between human vitreous RBP3 concentrations and HbA1c plotted with a regression line. n=55.

Figure S10

A



B



C

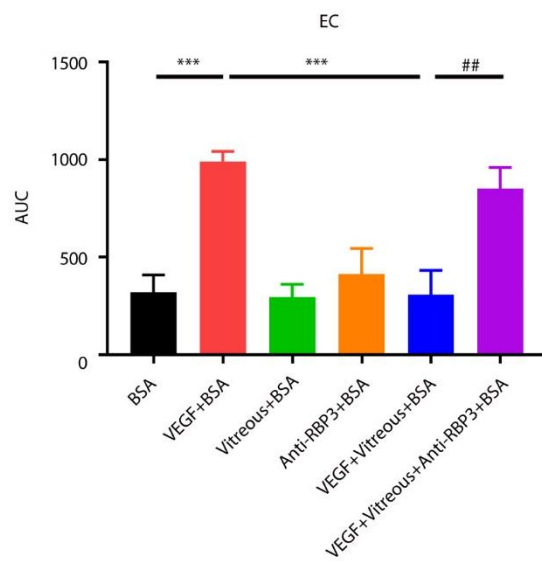


Fig. S10. Effects of rhRBP3 or Medalist patient vitreous from protected eye on endothelial migration.

Effects of rhRBP3 (0.25 μ g/mL, 2nM) or medalist patient vitreous from protected eye on 25mM glucose (HG) or rhVEGF (2.5ng/mL)-induced endothelial migration in bovine retinal endothelial cell (BREC). AUC for Fig. 5A-C. All data are represented as mean \pm SEM. Group comparison was done by ANOVA. (A) * p <0.05 versus HG; ^{##} p <0.01 versus HG+RBP3. n=4. (B) * p <0.05 versus VEGF; [#] p <0.05 versus VEGF+RBP3. n=4-5. (C) *** p <0.001 versus VEGF+BSA; ^{##} p <0.01 versus VEGF+Vitreous+BSA. n=3.

Table S1. Clinical and demographic characteristics by disease status for Medalist patients included in proteomic analysis by mass spectroscopy.

	No-mild NPDR	PDR
Total number	4	6
Number of medalist patients	4	6
	Percentage or Median [lower quartile, upper quartile]	
Age (years)	79 [65, 86]	77 [71, 78]
Gender (Female, %)	25.0%	33.3%
Type of diabetes (Type 1, %)	100%	100%
Duration of disease (years)	64 [53, 76]	67 [57, 72]
Age at diagnosis (years)	12 [6, 17]	8 [7, 10]
HbA1c (%)	7.3 [6.4, 8.2]	7.2 [6.6, 7.3]
BMI (kg/m ²)*	20.8 [17.8, 23.8] ^(2†)	27.8 [22.7, 30.4]
Total Cholesterol (mg/dL)	155 [129,179]	156 [131, 158]
Triglycerides (mg/dL)	71 [65, 86]	54 [43, 75]
HDL (mg/dL)	55 [49, 59]	62 [46, 75]
LDL (mg/dL)	83 [62, 108]	69 [65, 70]
CRP (mg/L)*	2.0 [0.6, 7.9]	1.8 [0.9, 3.3]
eGFR (ml/min /1.73m ²)*	59.4 [48.1, 73.4]	47.7 [43.2, 71.8]
Hypertension (%)*	50.0%	83.3%
Neuropathy (%)	75.0%	83.3%
CVD (%)	50.0%	100%

DM= diabetes mellitus. PDR= proliferative diabetic retinopathy. BMI= body mass index.

HDL= high-density lipoprotein cholesterol. LDL= low-density lipoprotein cholesterol.

CRP= C-reactive protein. eGFR= estimated glomerular filtration rate. CVD= cardiovascular disease.

*Available only in medalist patients. †Number lacking data. P-values were calculated by Kruskal-Wallis or Fisher's Exact Test.

Table S2. Four candidates of up-regulated proteins selected by proteomic analysis in retina and vitreous of Medalist patients with no-mild NPDR (*n* = 6, protected) versus PDR (*n* = 11, nonprotected). *p* < 0.05 cutoff by Mann–Whitney U test.

Protein Name	Retina		Vitreous	
	Fold change	P value	Fold change	P value
RBP3 Interphotoreceptor retinoid-binding protein precursor	1.61	0.0444	1.88	0.0049
PTPRZ1 Protein Tyrosine Phosphatase, Receptor Type Z1	1.33	0.0484	1.20	0.0480
PPME1 Isoform 3 of Protein phosphatase methylesterase 1	1.20	0.0484	1.17	0.0484
TNR Isoform 2 of Tenascin-R precursor	1.48	0.0496	1.54	0.0428

Table S3. RBP3 protein was selected from among the four candidates in table S2.

Protein Name	Retina <i>n</i> =17 eyes, 10 people				Vitreous <i>n</i> =17 eyes, 10 people			
	No-Mild NPDR <i>n</i> =6 eyes, 4 people	PDR <i>n</i> =11 eyes, 6 people	Fold-change (Mean)	P-value	No-Mild NPDR <i>n</i> =6 eyes, 4 people	PDR <i>n</i> =11 eyes, 6 people	Fold-change (Mean)	P-value
Retinol Binding Protein 3 (Interphotoreceptor retinoid-binding protein)								
Peptide hit numbers (Median)	414.5	268	1.61	0.04	560	269	1.88	<0.01

Total numbers of detected peptide hits of RBP3 were 318 (retina) and 327 (vitreous) in median of all subjects. The selecting criteria was a minimum 1.5-fold increase of peptide hit numbers with *p*-value <0.05 in both retina and vitreous. *P*-values were calculated using Mann–Whitney U test.

Table S4. Clinical and demographic characteristics by disease status for individuals included in proteomics and ELISA assays.

	Non-DM (NDM)	No-Mild NPDR	Moderate NPDR	#PDR
Total number (eyes, subjects)	17[13]	30[19]	9[8]	23[14]
Number of medalist patients	0	12	7	14
Number of non-medalist patients	13	7	1	0
	Percentage or Median [lower quartile, upper quartile]			
Age (years)	78 [73, 83] ^(1†)	81 [77, 86]	75 [64.5, 83.5]	76[73, 87]
Gender (Female, %)	50% ^(1†)	42.1%	50.0% ^o	57.1%
Type of diabetes (Type 1, %)*	N/A	68.4.%	100%	100%
Duration of disease (years)*	N/A	56 [35-60] ^(2†)	54.5[50.5-63.0]	63.5[57-75]
Age at diagnosis (years) **	N/A	20 [15-47] ^(3†)	13[6-18.5]	8[4-12]
HbA1c (%)	N/A	7.0 [6.5, 7.5] ^(3†)	7.4 [5.8, 8.4] ^(1†)	7.3 [7.1, 7.5]
BMI (kg/m ²) ^	N/A	25.1 [22.5, 29.0] ^(7†)	28.3 [23.8, 29.1] ^(2†)	26.6 [21.8, 32.4]
Total Cholesterol (mg/dL)	N/A	142 [122, 158] ^(4†)	138 [134, 162] ^(1†)	155 [135, 162]
Triglycerides (mg/dL)	N/A	80.5 [53, 137] ^(5†)	61 [41, 71] ^(1†)	64.5 [41, 83]
HDL (mg/dL)	N/A	51 [45, 70] ^(6†)	60 [59, 72] ^(1†)	61.5 [49, 75]
LDL (mg/dL)	N/A	66 [57, 76] ^(6†)	55 [52, 76] ^(1†)	74 [55, 89]
CRP (mg/L) ^	N/A	0.74[0.5-0.9] ^(7†)	1.00[0.6-1.3] ^(3†)	0.90 [0.6-3.3]
eGFR (ml/min /1.73m ²) ^	N/A	52.4 [41.7, 63.8] ^(7†)	59.3 [56.1, 60.9] ^(1†)	59.2 [45.6, 91.2]
Hypertension (%) ^	N/A	57.9% ^(5†)	75.0%	78.6%

Neuropathy (%)	N/A	47.3 ^(5†)	62.5%	64.3% ^(2†)
CVD (%)	N/A	42.1% ^(4†)	62.5%	92.9%

DM= diabetes mellitus. DR= diabetic retinopathy. NPDR= non-proliferative DR. PDR= proliferative DR. BMI= body mass index. HDL= high-density lipoprotein cholesterol. LDL= low-density lipoprotein cholesterol. CRP= C-reactive protein. eGFR= estimated glomerular filtration rate. CVD= cardiovascular disease. From 54 unique subjects, 2 medalist patients have different diabetic retinopathy grades in eyes. #All PDR are quiescent PDR. ^Available only in medalist patients. †Number lacking data. Group comparison was done by Kruskal–Wallis test and Chi-square test where applicable. *p < 0.05, **p < 0.01.

Table S5. Up-regulated proteins in the retina from Joslin Medalist patients: protected versus nonprotected.

Protein Name	Fold change	p value
COX5A Cytochrome c oxidase subunit 5A, mitochondrial precursor	1.81	0.001495
C3orf28 E2-induced gene 5 protein	2.20	0.002060
LGALS3 MGC148757 protein	0.29	0.002120
STX12 Syntaxin 12	1.81	0.002293
LOC644934 similar to ribosomal protein S26	1.53	0.002938
ATP5J ATP synthase, H ⁺ transporting, mitochondrial F0 complex, subunit F6 isoform b precursor	1.70	0.002970
HMOX2 Heme oxygenase 2	1.75	0.003361
- cDNA FLJ61278, highly similar to Protein-arginine deiminase type-2	0.45	0.003420
STX3 Isoform A of Syntaxin-3	1.59	0.003501
NDUFA4 NADH dehydrogenase [ubiquinone] 1 alpha subcomplex subunit 4	1.51	0.003666
PPA2 Isoform 1 of Inorganic pyrophosphatase 2, mitochondrial precursor	1.46	0.005624
NDUFA5 NADH dehydrogenase [ubiquinone] 1 alpha subcomplex subunit 5	1.48	0.006326
VDAC1 Voltage-dependent anion-selective channel protein 1	1.62	0.006656
CD44 Isoform 4 of CD44 antigen	0.48	0.007587
NDUFA6 NADH dehydrogenase (ubiquinone) 1 alpha subcomplex, 6, 14kDa	1.67	0.008046
DNAJC5 Isoform 1 of DnaJ homolog subfamily C member 5	1.95	0.008516
CST3;CST2 Cystatin-C precursor	1.86	0.008759
CRYAA Alpha-crystallin A chain	0.58	0.008889
ACTG1 Actin, cytoplasmic 2	0.68	0.008931
ABHD14B Isoform 1 of Abhydrolase domain-containing protein 14B	0.55	0.009089
ALDH9A1 4-trimethylaminobutyraldehyde dehydrogenase	0.62	0.010148
NDUFB6 NADH dehydrogenase [ubiquinone] 1 beta subcomplex subunit 6	1.44	0.011467
GOLPH3 Golgi phosphoprotein 3	1.33	0.012660

MRPS26 28S ribosomal protein S26, mitochondrial	1.30	0.012660
TOMM20 Mitochondrial import receptor subunit TOM20 homolog	1.73	0.012660
LRG1 Leucine-rich alpha-2-glycoprotein precursor	1.60	0.012660
AGT Angiotensinogen precursor	1.43	0.012660
PTMA Putative uncharacterized protein	1.50	0.012660
HMGN1 High-mobility group nucleosome binding domain 1	2.97	0.012660
UQCRB UQCRB protein	1.43	0.013171
PCCA propionyl-Coenzyme A carboxylase, alpha polypeptide isoform b	1.51	0.013996
LOC153364 Isoform 2 of Beta-lactamase-like protein FLJ75971	1.64	0.014325
MTX1 metaxin 1 isoform 1	1.57	0.014660
RGS9 Isoform 3 of Regulator of G-protein signaling 9	1.62	0.014930
DLAT Pyruvate dehydrogenase complex component E2	1.58	0.015224
BASP1 Brain acid soluble protein 1	1.48	0.015605
IDH3B Isocitrate dehydrogenase 3, beta subunit isoform a precursor	1.77	0.015605
VAMP2 Uncharacterized protein VAMP2	1.88	0.015797
NUCB1 Nucleobindin-1	1.75	0.016661
RHOG Rho-related GTP-binding protein RhoG	0.67	0.017257
LCN1 Lipocalin-1 precursor	1.49	0.017708
VDAC2 Voltage-dependent anion-selective channel protein 2	1.62	0.017831
CEND1 Cell cycle exit and neuronal differentiation protein 1	2.08	0.017989
RGR retinal G-protein coupled receptor isoform 1	0.41	0.018884
ARPC5L Actin-related protein 2/3 complex subunit 5-like protein	0.64	0.018958
NDUFA12 13kDa differentiation-associated protein variant (Fragment)	1.58	0.019871
RPS3 40S ribosomal protein S3	0.65	0.020179
PTGDS Prostaglandin D2 synthase 21kDa	1.91	0.020489
- Transthyretin	2.66	0.020489
CLTC Isoform 2 of Clathrin heavy chain 1	1.43	0.020800
KIAA1576 Probable oxidoreductase KIAA1576	0.55	0.023567
ACO2 Aconitase 2, mitochondrial	1.40	0.023653
NDUFB11 Isoform 2 of NADH dehydrogenase [ubiquinone] 1 beta subcomplex subunit 11, mitochondrial	1.81	0.024967

COX7A2 Uncharacterized protein COX7A2	2.24	0.025477
RAB6A Isoform 2 of Ras-related protein Rab-6A	0.81	0.025912
ACSL6 79 kDa protein	1.84	0.025912
REEP6 Receptor expression-enhancing protein 6	1.52	0.026749
ANXA1 Annexin A1	0.32	0.026843
PTBP1 Isoform 2 of Polypyrimidine tract-binding protein 1	0.63	0.028118
COX6B1 12 kDa protein	1.31	0.028230
PGM5 Isoform 2 of Phosphoglucomutase-like protein 5	0.70	0.028389
ATIC Bifunctional purine biosynthesis protein PURH	0.47	0.029383
HINT2 Histidine triad nucleotide-binding protein 2	1.70	0.029995
RAB18 Ras-related protein Rab-18	1.19	0.030402
RNF170 Isoform 5 of RING finger protein 170	0.73	0.031409
GPX3 Glutathione peroxidase 3 precursor	1.96	0.032084
IDH3G Isocitrate dehydrogenase [NAD] subunit gamma, mitochondrial	1.63	0.032084
EGFR Isoform 3 of Epidermal growth factor receptor	1.50	0.032198
NDUFA2 NADH dehydrogenase [ubiquinone] 1 alpha subcomplex subunit 2	1.34	0.033332
VCL Isoform 2 of Vinculin	0.57	0.033481
MTPN Myotrophin	0.71	0.033527
LARS2 Probable leucyl-tRNA synthetase, mitochondrial	1.31	0.033827
ATP5L ATP synthase subunit g, mitochondrial	1.44	0.034143
FHL1 Four and a half LIM domains 1	0.56	0.034253
BCL2L13 35 kDa protein	1.58	0.034253
UBC;UBB;RPS27A 79 kDa protein	1.69	0.034808
SELENBP1 54 kDa protein	0.56	0.034971
ACOX1 Isoform 2 of Peroxisomal acyl-coenzyme A oxidase 1	1.35	0.035440
FECH Ferrochelatase, mitochondrial precursor	1.46	0.036936
COX5B Cytochrome c oxidase subunit 5B, mitochondrial precursor	1.45	0.037093
LAP3 Isoform 2 of Cytosol aminopeptidase	0.66	0.038166
TPT1 Translationally-controlled tumor protein	0.67	0.038525
PRPF19 Pre-mRNA-processing factor 19	1.28	0.038765
TOMM70A Mitochondrial precursor proteins import receptor	1.53	0.038765
MSN Uncharacterized protein MSN (Fragment)	0.53	0.039126
COX4I1 Cytochrome c oxidase subunit 4 isoform 1, mitochondrial precursor	1.57	0.039247

GFM1 66 kDa protein	1.34	0.039857
NDUFA13 cell death-regulatory protein GRIM19	1.62	0.040425
GDPD1 Isoform 2 of Glycerophosphodiester phosphodiesterase domain-containing protein 1	1.49	0.042808
PTGES2 Prostaglandin E synthase 2	1.56	0.044033
MARCKS Myristoylated alanine-rich C-kinase substrate	1.60	0.044033
GSN Isoform 1 of Gelsolin precursor	0.62	0.044293
CNDP2 Cytosolic non-specific dipeptidase	0.68	0.044293
GOT2 Aspartate aminotransferase, mitochondrial precursor	1.60	0.044423
RBP3 Interphotoreceptor retinoid-binding protein precursor	1.61	0.044423
MXRA7 Isoform 3 of Matrix-remodeling-associated protein 7	1.65	0.045588
SPCS2 hypothetical protein	0.69	0.046530
LYPLA1 Isoform 2 of Acyl-protein thioesterase 1	1.32	0.047223
NDUFB4 Putative uncharacterized protein (Fragment)	1.42	0.047706
BCAM basal cell adhesion molecule isoform 2 precursor	0.69	0.047779
BCS1L Mitochondrial chaperone BCS1	1.20	0.047968
COL3A1 Isoform 1 of Collagen alpha-1(III) chain	1.13	0.047968
PDCD5 Programmed cell death protein 5	1.13	0.047968
PCDH1 protocadherin 1 isoform 1 precursor	1.20	0.047968
TST Thiosulfate sulfurtransferase	1.20	0.047968
RHOT1 ras homolog gene family, member T1 isoform 2	1.20	0.047968
CCDC47 Isoform 2 of Coiled-coil domain-containing protein 47	1.13	0.047968
HSPA4L cDNA FLJ55529, highly similar to Heat shock 70 kDa protein 4L	1.13	0.047968
RABL4 Protein	1.13	0.047968
SNRPD1 16 kDa protein	1.53	0.047968
IPIr00871555	1.27	0.047968
GAA acid alpha-glucosidase preproprotein	1.24	0.048058
EIF3D Eukaryotic translation initiation factor 3 subunit D	1.17	0.048406
SEPT4 cDNA FLJ55761, highly similar to Septin-4	1.17	0.048406
DNAJA1 DnaJ homolog subfamily A member 1	1.30	0.048406
LETM1 Leucine zipper-EF-hand-containing transmembrane protein 1, mitochondrial precursor	1.33	0.048406
SLC4A7 Isoform 3 of Sodium bicarbonate cotransporter 3	1.37	0.048406
TRIM36 Tripartite motif-containing protein 36	1.17	0.048406
MLF2 Myeloid leukemia factor 2	1.17	0.048406

M6PR Cation-dependent mannose-6-phosphate receptor	1.33	0.048406
- 22 kDa protein	1.17	0.048406
TMEM109 Transmembrane protein 109 precursor	1.37	0.048406
MAP4 Isoform 3 of Microtubule-associated protein 4	1.17	0.048406
PCNP Isoform 2 of PEST proteolytic signal-containing nuclear protein	1.23	0.048406
TXNDC10 Isoform 1 of Protein disulfide-isomerase TXNDC10	1.17	0.048406
UBQLN1 Isoform 1 of Ubiquilin-1	1.40	0.048406
CHMP5 Charged multivesicular body protein 5	1.20	0.048406
LOC255374 Beta-lactamase-like protein LOC255374	1.37	0.048406
PCP2 Purkinje cell protein 2 homolog	1.47	0.048406
H2AFZ Histone H2A.Z	1.27	0.048406
FABP3 Fatty acid-binding protein, heart	1.30	0.048406
CRYBA2 Beta-crystallin A2	1.17	0.048406
FRZB Secreted frizzled-related protein 3	1.47	0.048406
LSM4 U6 snRNA-associated Sm-like protein LSM4	1.27	0.048406
CHMP6 Charged multivesicular body protein 6	1.40	0.048406
RGS9BP Regulator of G-protein signaling 9-binding protein	1.27	0.048406
IPI00396023	1.27	0.048406
PPME1 Isoform 3 of Protein phosphatase methylesterase 1	1.20	0.048406
ATP6V1H Isoform 2 of Vacuolar proton pump subunit H	1.27	0.048406
MAP6 Isoform 1 of Microtubule-associated protein 6	1.43	0.048406
TCEAL3 Transcription elongation factor A protein-like 3	1.50	0.048406
CPLX3 Complexin-3	1.33	0.048406
TARS2 Threonyl-tRNA synthetase, mitochondrial	1.20	0.048406
SURF4 Surfeit 4	1.23	0.048406
SNRPC Small nuclear ribonucleoprotein polypeptide C	1.57	0.048406
PPIH Peptidyl-prolyl cis-trans isomerase	1.27	0.048406
CTPS2 CTP synthase 2	1.23	0.048406
TIMM50 Isoform 1 of Mitochondrial import inner membrane translocase subunit TIM50	1.30	0.048406
LOC650883 similar to KIAA1990 protein	1.17	0.048406
INSR insulin receptor isoform Short precursor	1.23	0.048406
GAP43 24 kDa protein	1.17	0.048406
PNPLA6 Isoform 1 of Neuropathy target esterase	1.20	0.048406
SLC25A36 Isoform 3 of Solute carrier family 25 member 36	1.20	0.048406
- PC1/MRPS28 fusion protein	1.23	0.048406

PTPRZ1 265 kDa protein	1.33	0.048406
- cDNA FLJ60514, highly similar to Fructosamine-3-kinase	1.37	0.048406
TNR Isoform 2 of Tenascin-R precursor	1.48	0.049596
NSDHL Sterol-4-alpha-carboxylate 3-dehydrogenase, decarboxylating	1.22	0.049715
CLSTN1 Isoform 1 of Calsyntenin-1 precursor (Fragment)	1.45	0.049969
PODXL podocalyxin-like isoform 1 precursor	1.35	0.049969
CCDC90B Isoform 2 of Coiled-coil domain-containing protein 90B, mitochondrial	1.46	0.049969

Joslin medalist patients with no-mild NPDR (n=6, Protected) vs. PDR (n=11, Non-protected). Values are expressed as fold change and p value was calculated using Mann–Whitney U test. The data are sorted by P value using $p < 0.05$ cut off.

Table S6. Up-regulated proteins in the vitreous from Joslin Medalist patients: protected versus nonprotected.

Protein Name	Fold change	p value
HMGB1 High-mobility group box 1	1.90	0.00294
XRCC5 Putative uncharacterized protein XRCC5	3.33	0.00297
- cDNA FLJ59582, highly similar to Ras-related protein Rab-3A	2.60	0.00297
RBP3 Interphotoreceptor retinoid-binding protein precursor	1.88	0.00487
APLP2 Isoform 1 of Amyloid-like protein 2 precursor	3.07	0.00536
CHL1 Isoform 1 of Neural cell adhesion molecule L1-like protein precursor	1.62	0.00564
NCL Isoform 2 of Nucleolin	1.77	0.00876
OTUB1 Isoform 1 of Ubiquitin thioesterase OTUB1	1.83	0.00876
CFD Complement factor D preproprotein	0.54	0.00876
SNCB Beta-synuclein	2.45	0.00882
SEZ6 Isoform 3 of Seizure protein 6 homolog precursor	1.77	0.00882
OLA1 Isoform 1 of Obg-like ATPase 1	1.49	0.01043
ST13 Hsc70-interacting protein	1.48	0.01050
PFKL cDNA FLJ30173 fis, clone BRACE2000969, highly similar to 6-phosphofructokinase, liver type	1.54	0.01050
FKBP3 FK506-binding protein 3	1.27	0.01254
ARL3 ADP-ribosylation factor-like protein 3	1.33	0.01254
MAPRE3 25 kDa protein	1.37	0.01254
AARS Alanyl-tRNA synthetase, cytoplasmic	1.61	0.01263
ARPC2 Actin-related protein 2/3 complex subunit 2	1.40	0.01266
SH3GL2 Endophilin-A1	1.67	0.01266
RAB11B Ras-related protein Rab-11B	1.50	0.01266
CNTN1 Isoform 2 of Contactin-1 precursor	1.60	0.01266
- cDNA FLJ59539, highly similar to Secernin-1	1.40	0.01266
PCBP1 Poly(rC)-binding protein 1	1.67	0.01266
- 18 kDa protein	1.30	0.01266
SPON1 Spondin-1 precursor	1.96	0.01640
APEX1 DNA-(apurinic or apyrimidinic site) lyase	2.32	0.01782
TAGLN Transgelin	2.43	0.01782
HSPA4 Heat shock 70 kDa protein 4	2.34	0.01857
LOC646817 similar to template activating factor-I alpha	1.83	0.01857

B3GNT1 N-acetyllactosaminide beta-1,3-N-acetylglucosaminyltransferase	1.92	0.01921
GLOD4 Isoform 2 of Glyoxalase domain-containing protein 4	1.63	0.02093
BTD Uncharacterized protein BTD (Fragment)	1.59	0.02210
FGB Fibrinogen beta chain precursor	1.93	0.02564
LGALS3BP Galectin-3-binding protein precursor	1.28	0.02878
COL18A1 Isoform 2 of Collagen alpha-1(XVIII) chain precursor	1.62	0.02945
NRCAM Isoform 3 of Neuronal cell adhesion molecule precursor	1.98	0.02945
hCG_1983058 hypothetical protein LOC644820	1.42	0.03186
SOD3 Extracellular superoxide dismutase [Cu-Zn] precursor	2.06	0.03252
APLP1 amyloid precursor-like protein 1 isoform 1 precursor	2.02	0.03321
CUTA Isoform B of Protein CutA precursor	1.31	0.03384
SH3BGRL 13 kDa protein	1.27	0.03384
PLG Plasminogen precursor	0.53	0.03425
A2M Alpha-2-macroglobulin precursor	1.71	0.03481
FCGBP IgGfC-binding protein precursor	2.98	0.03757
LRP2 Low-density lipoprotein receptor-related protein 2 precursor	1.75	0.03943
OAF Out at first protein homolog precursor	2.13	0.03943
ANP32A ANP32A protein (Fragment)	1.92	0.03943
HNRNPD HNRPD protein	1.99	0.03943
DPYSL3 Dihydropyrimidinase-related protein 3	2.37	0.03943
TIMP2 22 kDa protein	1.37	0.04203
CLEC3B Putative uncharacterized protein DKFZp686H17246	0.51	0.04209
ACP1 Acid phosphatase 1, soluble	1.49	0.04219
PPP1R7 Isoform 1 of Protein phosphatase 1 regulatory subunit 7	1.29	0.04258
HDHD2 Isoform 1 of Haloacid dehalogenase-like hydrolase domain-containing protein 2	1.43	0.04258
ATP6V1E1 Vacuolar proton pump subunit E 1	1.83	0.04281
TNR Isoform 2 of Tenascin-R precursor	1.54	0.04281
EIF4A2 Isoform 1 of Eukaryotic initiation factor 4A-II	1.97	0.04283
TKT Transketolase variant (Fragment)	2.54	0.04283
NCAM1 neural cell adhesion molecule 1 isoform 2	1.39	0.04523

MAT2B Isoform 1 of Methionine adenosyltransferase 2 subunit beta	1.13	0.04797
NSF Vesicle-fusing ATPase	1.13	0.04797
C6orf108 c-Myc-responsive protein Rcl	1.27	0.04797
PURA Transcriptional activator protein Pur-alpha	1.20	0.04797
GALM Aldose 1-epimerase	1.33	0.04797
COPS8 COP9 signalosome subunit 8 isoform 2	1.20	0.04797
GNB3 GNB3 protein	1.47	0.04797
PSMD1 Isoform 2 of 26S proteasome non-ATPase regulatory subunit 1	1.33	0.04797
MYH10 Isoform 2 of Myosin-10	1.13	0.04797
CACYBP cDNA FLJ36106 fis, clone TEST12021531, highly similar to Calcyclin-binding protein	1.33	0.04797
PSMA4 26 kDa protein	1.20	0.04797
PTPRZ1 265 kDa protein	1.20	0.04797
SEPT7 Putative uncharacterized protein DKFZp5861031	1.13	0.04797
CLIC5;LOC100131610 chloride intracellular channel 5 isoform a	1.13	0.04797
ACTR2 Actin-related protein 2	1.23	0.04841
LANCL1 LanC-like protein 1	1.17	0.04841
HDGFRP3 Hepatoma-derived growth factor-related protein 3	1.30	0.04841
ATP6V1B2 Vacuolar ATP synthase subunit B, brain isoform	1.30	0.04841
PTPLAD1 Protein tyrosine phosphatase-like protein PTPLAD1	1.17	0.04841
NAPA Alpha-soluble NSF attachment protein	1.23	0.04841
CTSL1 Cathepsin L1 precursor	1.20	0.04841
UNC119 Isoform A of Protein unc-119 homolog A	1.40	0.04841
SEZ6L2 Isoform 3 of Seizure 6-like protein 2	1.17	0.04841
NDRG1 Protein NDRG1	1.33	0.04841
USO1 Putative uncharacterized protein DKFZp451D234	1.37	0.04841
FDPS Farnesyl diphosphate synthase	1.23	0.04841
LXN Latexin	1.27	0.04841
HEBP1 Heme-binding protein 1	1.23	0.04841
SFRS1 Isoform ASF-1 of Splicing factor, arginine/serine-rich 1	1.40	0.04841
APRT Adenine phosphoribosyltransferase	1.23	0.04841
PSMA2 Proteasome subunit alpha type-2	1.30	0.04841
CALB1 Calbindin	1.33	0.04841

SERPINA7 Thyroxine-binding globulin	1.47	0.04841
BLVRA Biliverdin reductase A precursor	1.47	0.04841
NONO Non-POU domain-containing octamer-binding protein	1.53	0.04841
XPOT Exportin-T	1.23	0.04841
TARS Threonyl-tRNA synthetase, cytoplasmic	1.27	0.04841
ACLY ATP citrate lyase isoform 2	1.23	0.04841
PPME1 Isoform 3 of Protein phosphatase methylesterase 1	1.17	0.04841
AP1B1 Isoform B of AP-1 complex subunit beta-1	1.23	0.04841
MAP2 Isoform 3 of Microtubule-associated protein 2	1.37	0.04841
FLNB Filamin B	1.30	0.04841
PSMD13 HSPC027	1.20	0.04841
PGM2 Phosphoglucomutase-2	1.47	0.04841
TPP2 Tripeptidyl peptidase II	1.53	0.04841
ANP32E Acidic	1.47	0.04841
HNRNPU cDNA FLJ54020, highly similar to Heterogeneous nuclear ribonucleoprotein U	2.07	0.04841
PACSIN1 Protein kinase C and casein kinase substrate in neurons 1	1.30	0.04841
PHYHIPL Isoform 2 of Phytanoyl-CoA hydroxylase-interacting protein-like	1.23	0.04841
SUB1 LOC533984 protein	1.40	0.04841
EIF3B Isoform 2 of Eukaryotic translation initiation factor 3 subunit B	1.17	0.04841
FAM169A Isoform 1 of UPF0611 protein FAM169A	1.23	0.04841
LOC652147 hypothetical protein, partial	1.17	0.04841
GARS Glycyl-tRNA synthetase	1.27	0.04841
KTN1 kinectin 1 isoform b	1.33	0.04841
IGLV1-40 V1-13 protein (Fragment)	1.30	0.04841
SNX3 Isoform 1 of Sorting nexin-3	1.17	0.04841
TXNL1 hypothetical protein LOC509142	1.30	0.04841
ANP32B 29 kDa protein	1.23	0.04841
PGM1 65 kDa protein	1.20	0.04841
GNB2L1 Guanine nucleotide-binding protein subunit beta-2-like 1	1.23	0.04841
KHSRP Isoform 2 of Far upstream element-binding protein 2	1.20	0.04841
AKAP12 Isoform 2 of A-kinase anchor protein 12	1.43	0.04841

ILF2 Interleukin enhancer binding factor 2 variant (Fragment)	1.23	0.04841
DNM1 Isoform 2 of Dynamin-1	1.37	0.04841
- cDNA FLJ59206, highly similar to Eukaryotic translation initiation factor 4B	1.30	0.04841
- cDNA FLJ51276, highly similar to Secretogranin-2	1.33	0.04841
SERPINI1 Neuroserpin precursor	1.58	0.04997

Joslin medalist patients with no-mild NPDR (n=6, Protected) vs. PDR (n=11, Non-protected). Values are expressed as fold change and p value was calculated using Mann–Whitney U test. The data are sorted by P value using $p < 0.05$ cut off.

Table S7. Primers sequences used in reverse transcription polymerase chain reaction.

Gene	Primers (5'-3')		Access Number
<i>18s</i>	F	GCTTAATTTGACTCAACACGGGA	NR_003278.3
	R	AGCTATCAATCTGTCAATCCTGTC	
<i>Vegf</i> (rat, mouse)	F	CTCGCAGTCCGAGCCGGAGA	NM_001204384.1
	R	GGTGCAGCCTGGGACCACTTG	
<i>Vegf</i> (bovine)	F	TACCCAGATGAGATTGAGTT	NM_001287044.1
	R	CCTTGCTTTATCTTTCTTTG	
<i>Il6</i> (rat)	F	TGATGCACTGTCAGAAAACA	XM_011515390.2
	R	ACCAGAGCAGATTTTCAATAGGC	
<i>Il6</i> (mouse)	F	ACCAGAGGAAATTTTCAATAGGC	NM_001314054.1
	R	TGATGCACTTGCAGAAAACA	
<i>Il6</i> (bovine)	F	GATGACTTCTGCTTTCCCTACC	XM_019959556.1
	R	TTGTGGCTGGAGTGGTTATTAG	
<i>Glut-1</i> (rat)	F	TGATTGGTTCCTTCTCTGTGG	NM_006516.2
	R	CCCAGGATCAGCATCTCAAAG	
<i>Glut-4</i> (rat)	F	ACTGGTCCTTGCTGTATTCTC	NM_001042.2
	R	CCAAGTTGCATTGTAGCTCTG	
<i>Sglt-1</i> (rat)	F	TCCCTATTTACATCAAGGCTGG	XM_011530331.1
	R	GGACAGAACGGAAAGGTAGATC	
<i>Sglt-2</i> (rat)	F	TTCCTCACACTCGCAATCTC	NM_022590.2
	R	CCTCTAACTCTTCAGCATCCAG	
<i>Rbp3</i> (retinol binding protein 3, interstitial) (mouse)	F	AGAGCACAAGGCTGAGATGG	NM_015745.2
	R	CTCCGAGCTGCTGGTAGAAC	